ON THE SIZE AND SHAPE OPTIMIZATION OF TRANSMISSION LINE TOWERS CONSIDERING BOLT SLIPPAGE

Rafael Souza

Leandro Miguel

souza.rafael.rodrigues@gmail.com — leandro.miguel@ufsc.br

CORE. UFSC - Rua Joao Pio Duarte, 88037-000. Florianopolis, SC, Brazil.

Joao Kaminki Junior

jkj@ufsm.br - UFSM - Av. Roraima, 1000, 97105-900. Santa Maria , RS, Brazil

Rafael Holddorf Lopez

rafael.holdorf@ufsc.br - Federal University of Santa Catarina - UFSC

Andre Jacomel Torii

ajtorii@hotmail.com - UFB - Cidade Universitria, 58051-900 s/n - Castelo Branco III, Joo Pessoa, PB, Brazil.

Abstract. *The current practice for structural design of transmission towers, adopts in general, linear-elastic models (or geometrical non-linear) and 3D truss or space frame elements. However, it is recognized by engineers that some non-linear effects may appear, mostly related to the actual behavior of the connections, more specifically, the bolt slippage effect. Since the significance of such effect increases with the structural stiffness, it is possible to avoid the demand for a more complex structural analysis, by prioritizing flexible designs. Notwithstanding, it is unclear if a more complex (and costly) analysis of a stiffer structure, can lead to a better design, in comparison to a simpler analysis of a more flexible structure. In order to address this question, this paper presents a comparison between the optimization of two structures on CIGRE (2009). Where, Structure 1 is the more flexible, and have small differences from Structure 2. Although slightly, these differences increase the stiffness and consequently the bolt slippage effect. The results indicated that the consideration of the bolt slippage allows the algorithm to reach a competitive optimum design, and in some cases, eve better ones, in comparison to the structures where these effects are not significant.*

Keywords: *Transmission tower structure; bolt slippage effect; Size and shape optimization; heuristic algorithm*

1 INTRODUCTION

Over the last few decades the structural optimization of trusses has been widely studied (Dorn (1964), Sved and Ginos (1968), Dobbs and Felton (1969), Pedersen (1972), Hemp (1973), Goldberg and Samtani (1986),Rajeev and Krishnamoorthy (1992), Camp and Farshchin (2014), Wu and Chow (1995), Galante (1996), Tang et al. (2005), Kelesoglu (2007), Grierson and Pak (1993), Rajan (1995), Hajela and Lee (1995), Rahami et al. (2008), Torii et al. (2012), Miguel et al. (2013), Wang and Ohmori (2013), Torii et al. (2014)).

Trusses are particularly target of structural optimization problems, because if compared with other type of structures, have a relatively simple analysis Šilih et al. (2010). Additionally, they are largely used in real life engineering, e.g. roofs, bridges, buildings, transmission towers, etc. A special attention can be given to transmission towers, since, in contrast to other structures that are generally unique, the same design of a specific tower is frequently built up to a hundreds of times in a single transmission line. Thus, cost savings and performance improvements of optimization procedures can have a large impact in the entire transmission line.

On the subject of structural optimization of transmission towers the following papers can be cited: Mathakari et al. (2007), Kaveh et al. (2008), Noilublao and Bureerat (2011). On the context of optimization focusing on industrial application, Shea and Smith (2006) and Guo and Li (2011) present the size, shape and topology optimization of a transmission tower. de Souza et al. (2016) presents the size, shape and topology optimization, where the topology is varied through a template strategy. Tort et al. (2017) present the size and shape optimization of transmission tower using a commercial software in order to evaluate the constraints.

On the context of structural behavior, the current industrial practice for structural design of transmission line steel towers usually adopts linear-elastic (or geometrical non-linear) analysis using 3D-truss or space frame elements. Despite the simple model employed, it has been recognized by engineers that some sources of non-linear effects may appear, mainly associated to the actual behavior of the tower connections, more specifically, the bolt slippage. (Al-Bermani and Kitipornchai (1990), Kitipornchai et al. (1994), Kroeker (2000), Ungkurapinan et al. (2003), Ahmed (2007), Kaminski-Jr (2007)).

CIGRE (2009) presents the model and experimental results for three towers (Towers 1, 2 and 2A). It also shows that, for some members of the stiffer structures, the results of the linear-elastic models are discrepant with respect to the experimental data. On the other hand, for the models including the bolt slippage effect, these discrepancies were reduced. The conclusions from CIGRE (2009) highlighted that, for some structures, it is necessary to consider in the model the bolt slippage effect.

Since the significance of such effect increases with the structural stiffness, it is possible to avoid the demand for a more complex structural analysis, by prioritizing flexible designs. In order to investigate if a stiffer structure (which demands a more complex, and costly, analysis) can lead to a better design, in comparison to a more flexible structure with a simpler analysis. This paper presents a comparison between the optimization of two transmission towers presented on CIGRE (2009). Where, Structure 1 is the more flexible structure, and have small differences from Structure 1. Although slightly, these differences increase the stiffness and consequently the bolt slippage effect. Consequently, these towers demand a more complex analysis.

Three cases are studied: (i) size and shape optimization of Structure 1, not considering the bolt slippage effect; (ii) size and shape optimization of Structure 2, not considering the bolt slippage effect; (iii) size and size and shape optimization of Structure 2, considering the bolt slippage effect. The results for all cases are presented and discussed.

2 IMPACT OF TOPOLOGY ON STRUCTURAL BEHAVIOR OF TRANSMISSION LINE TOWERS

One of the first experimental investigations carried out to better understand the structural behavior of transmission line towers was promoted by CIGRE (1991). A prototype structure was constructed and some internal member forces were measured. These results showed important discrepancies among the predictions provided by a group of 27 international designers. Moreover, the predictions among the engineers themselves also presented important divergences, due to their distinct modeling assumptions.

A new experiment was proposed by CIGRE (2009). Three new prototype structures with small differences in their topologies were constructed and tested. Although these differences were slight, they played an important role in the stiffness of the structures. Despite the discrepancies decreased, they were still present in some diagonals of the two stiffer structures, while in the most flexible prototype the internal forces were coincident.

Then, using the experimental load-slip relationship results of typical tower angles determined by Ungkurapinan et al. (2003), CIGRE (2009) modeled the connections of the prototype structures tested as nonlinear springs. The results were compared to the monitored data, showing that the structural prediction of the two stiffer structures approached the experimental observation.

The second CIGRE (2009) experimental investigation confirmed what tower design engineers believed, based on their observations of full-scale tower testing: the more the structural stiffness increases, the more the bolt slippage impacts on the tower behavior. In addition, predictions made by simple models are more discrepant in some members as the structural stiffness increases. Because the topology is directly related to the tower stiffness, the structural configuration chosen by the designer has great influence in the degree of convergence between the theoretical predictions and the measured results obtained in the tests.

Observe in Figure 1 the differences in the diaphragms position and in the diagonals configuration in Models 1 and 2. The diagonals configuration between the inclined and straight tower bodies as well as the cross-sectional configuration shown in Section M2 provide to the Model 2 a significant increase in its stiffness. Indeed, diagonal edges in ”X” configuration provide an increment in tower stiffness. Therefore, it would not be indicated that the transitions between the inclined and the straight tower bodies be done with ”X” diagonal in both tower faces. In practice, it is recommended that this transition be similar to the one presented in Model 1. In addition, it is recommended that the diaphragm should be located in the superior part of the extension (as it is shown in Section M1).

Consequently, if the designer takes these premises into account in the topology definition, at least in some degree, the theoretical predictions carried out by simple models would be more liable to the actual structural behavior.

Thus, it was recommended to designers a careful attention in the topology definition, mainly observing details that could contribute to increase the structural stiffness. In practice,

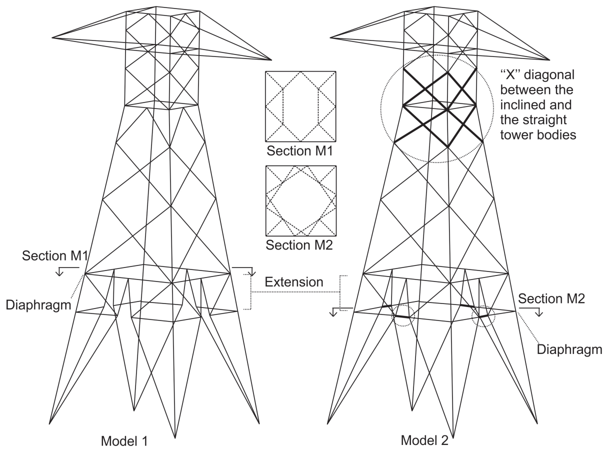

Figure 1: Difference on the topology of transmission line towers

simple aspects as the position of the diaphragms and the diagonals configuration would be enough the make the tower more flexible and, thus, less prone to the bolt slippage effects.

3 TRANSLATION IN BOLTED CONNECTIONS

In transmission line towers the connections are made as contact type connections, using galvanized bolts. According to CIGRE (2009) and Kaminski-Jr (2007), even though minimum and maximum tightening torques are recommended, the resistance to the sliding between the connected parts is not considered in the dimension of the connection.

The total translation deformation in a bolted connection includes the deformation of the connector, that is, of the bolt rod, the sliding deformation and the profile deformation at the bolt hole. Among all these deformations, the most significant one is the sliding deformation. Since, it occurs on a low level load, besides increasing the structure capacity to support differential movements at the foundations, because allows a redistribution of the loads on the tower members.

As previously mentioned, Ungkurapinan et al. (2003) tested a typical tower connection, using single angle profiles and aligned bolts, as show in Fig. 2. The results allowed them to reach an experimental load-slip relationship, which can be represented by the graphic on Fig. 3. Where the curve represents the behavior of the total deformation of the bolted connection (δ) as a function of the applied load (F).

Figure 3 presents four disguised regions:

- **Region 1:** the applied load (F) does not surpass the sliding resistance. There are only displacements related to the elastic deformation of the profiles. Even though there is no specification for the assembly torque (bolt tightening) in the contact type connections, there is always a sliding resistance between the connected angles at the beginning of load application. Thus, the inclination θ is highly dependent on the tightening torque.
- **Region 2:** the applied load (F) surpasses the sliding resistance. A rough displacement occurs caused by the sliding between the profiles until the accommodation of the bolts at their respective holes. Consequently, the displacement (P) is governed by the assembly clearance;

- **Region 3:** the hole is elastically deformed, and consequently the load-displacement ratio remains linear. Since, in this region, the hole is in direct contact with the hole wall, the displacement (Q) is highly dependent on the respective contact area, i.e. the bolt diameter and the profile thickness;
- **Region 4:** an inelastic deformation of the bolts and angles occurs, culminating in a failure of the connection.

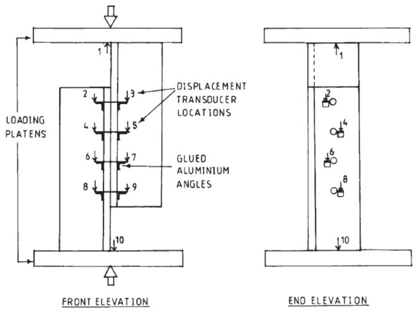

Figure 2: Connection composed by single angles and aligned bolts, tested in Ungkurapinan et al. (2003)

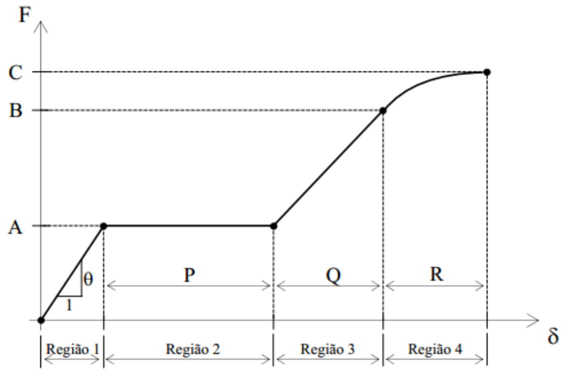

Figure 3: Applied force and total deformation relationship.

3.1 Modeling of the bolt slippage effect

The translation deformation on a bolted connection, discussed previously, is now introduced on a mechanical model. To do so, springs (with a non linear force-deformation relationship) are introduced, as illustrated on Fig. 4. On the left, there is the model without the bolt slippage, where all members are modeled as space frame elements. On the right, is illustrated how the connection between the horizontal (H1) and the main bar would be modeled. On each connection, a new node is created (e.g. node *3'*). Now, the H1 member is connected to the node *3'*, and a spring connects the nodes *3'* and *1*. It is important to highlight that the new nodes are created with the same coordinate of its respective connection, thus: coordinates *1* and *3'*, as well as *2* and *4'* are coincident.

The analysis is performed through ANSYS, employing BEAM4 elements for the space frame elements and COMBIN39 for the non-linear springs. The COMBIN39 is set as unidirectional elements with only one degree of freedom (translation in the x, y or z directions).

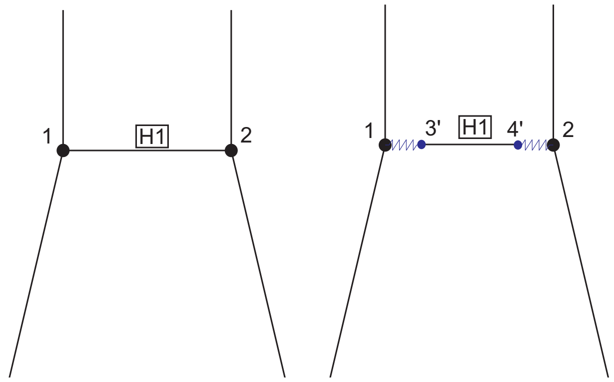

Figure 4: Illustration on how the springs are introduced

Thus, three COMBIN39 elements are introduced on each connection in order to represent the translation in x, y and z.

The non-linear springs, introduced between the nodes of the elements, are characterized by load versus displacement curves, similar to Fig. 3. Ungkurapinan et al. (2003) provide an load-displacement relationship (presented on Fig. 5), experimentally based, for an angle profile *L 102 x 102 x 6.4mm*, with 1 to 4 aligned bolts of 16mm of diameter, tightening torque of 114.28kN.mm and assembly clearance of 1.6mm.

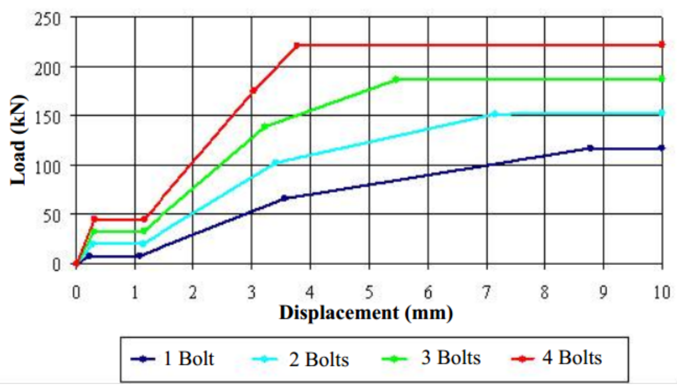

Figure 5: Load-displacement relationship considering an *L 102 x 102 x6.4mm* profile and a tightening torque of 114.28kN.mm.

Although the load-displacement relationship on Fig. 5 is valid only for the respective profile under the mentioned characteristics. Ungkurapinan et al. (2003) state the feasibility of interpolation of the load-deformation relationship for joints similar in configuration but differing in number of bolts. The authors present load-deformation expressions for different regions in terms of number of bolts.

Using these equations, the curves were adjusted to the profiles and bolts employed on the studied towers. In addition to the number of bolts, the cross sectional area, the contact area between the profiles and the bolts, the assembly clearance regarding the bolt and hole diameters and the tightening of the bolts were also taking into consideration in order to adjust the curves to the desirable profiles.

The analysis is linear, physical and geometrical. However, as shown in Figs. 5 and 3, the sprigs present a non-linear force-displacement relationship, for that reason an iterative process is employed. Highlighting that no conventional geometrical and physical non-linearities are employed.

These non-linear springs are inserted in all connections between: (i) diagonal and main bars; (ii) diagonals and horizontal bars; and (ii) horizontal bars and main bars.

Since the translation deformation occurs on each axis: ”x”, ”y” and ”z”, the adjusted force-displacement curves need to be decomposed. This is achieved by multiplying the respective curve by the directing cosine of the element in the corresponding direction.

4 DESIGN OF THE BOLTED CONNECTIONS

The current literature on transmission line tower optimization, even the ones that focuses on industrial application (Sivakumar et al. (2004), Mathakari et al. (2007), Kaveh et al. (2008), Noilublao and Bureerat (2011), Mathakari et al. (2007), Shea and Smith (2006), de Souza et al. (2016)) ignores the design of the connections. Mostly because it is a secondary design step and highly dependent on the designers choice. However, the number of bolts modifies the net area of the profile and consequently its tension capacity. Since optimal structures tend to work very close to full capacity, the correct design of the number of bolts can have a significant impact on the optimization process. Considering these aspects, on this paper the number of bolts is evaluated on each possible design generated by the algorithm.

Additionally, hence the main goal of this paper is to compare the optimization of a more flexible structure using a simpler analysis with a more rigid structure using an analysis that considers the bolt slippage effect. Since the modeling of this effect is significantly related to the number of bolts, it is indispensable that on each structure the force-displacement curves are correctly defined.

The horizontal and vertical hole-hole and hole-edge distances are mostly a designers choice. Thus, a few real design were studied in order to create an appropriate pattern. The number of bolts was determined following the recommendations of the NBR:8850 (2003). Where the connections are verified for the combined action of shear and axial stresses on the bolts and the bearing resistance of the members.

Since the structure is submitted to two load cases and the members are divided into groups, the final number of bolts is chosen as the maximum value among the members on every group, considering both load cases. Additionally, it is important to highlight that the leg members are connected on both flanges, thus, the number of bolts on their groups is always a multiple of two.

5 OPTIMIZATION PROBLEM

During the process, the optimization variables are stored in the vector $\mathbf{x}$. For size optimization the cross sectional areas of the structural members are taken as the design variables, represented as the vector $\mathbf{a}$. The coordinates of some chosen nodes are taken as design variables for shape optimization, and stored in vector $\boldsymbol{\xi}$. For practical purposes, the design variables related to nodal coordinates are taken as discrete values, rounded into centimeters. The final vector of design variables is $\mathbf{x} = \{\mathbf{a}, \boldsymbol{\xi}\} = \{a_1, \ldots, a_m, \xi_1, \ldots, \xi_q\}$, where m is the number of cross-sectional areas and q is the number of nodal coordinates taken as design variables.

The aim of the optimization problem is to minimize the structural weight while respecting the imposed constraints. Therefore, the problem can be written as Eq. 1:

$$\begin{aligned}
&\textbf{Find} \quad \mathbf{x} = \{a_1, \ldots, a_m, \xi_1, \ldots, \xi_q\} \\
&\textbf{That minimizes} \;\; w = \sum_{i=1}^{m} \rho_i l_i(\mathbf{x}) a_i(\mathbf{x}) \\
&\textbf{Subjected to load constraints} \\
&g_i(\mathbf{x}) = |S_{di}(\mathbf{x})| - R_{di} \leq 0, \;(i = 1, 2, \ldots, m), \\
&\textbf{Slenderness constraints} \\
&g_{i+m} = \lambda_t(\mathbf{x}) - \bar{\lambda}_t \leq 0, \;(i = 1, 2, \ldots, m) \\
&\textbf{and cross sectional constraints} \\
&g_{i+2m}(\mathbf{x}) = \frac{w_i(\mathbf{x})}{t_i(\mathbf{x})} - w/t_{max}
\end{aligned} \tag{1}$$

where W is the structural weight, and for a given bar i, ρ_i is the specific weight of the material, l_i is the length of each bar, S_{di} is the factored load in each bar, R_{di} is the factored resistance of each bar, λ_i is the slenderness ratio of each bar, $\bar{\lambda}_i$ is the allowable slenderness ratio of each bar, t_i is the thickness of each bar, w_{fi} is the flat width of each angle profile leg and w_f/t_{max} is the allowable relation between w and t for each bar.

The allowable stress of each bar $\bar{\sigma}_i$ is calculated following the recommendations of ASCE:10-15 (2015), considering whether the bar is under tension or compression (also taking into account local buckling). The allowable slenderness ratios $\bar{\lambda}_i$ are also calculated following the recommendation of ASCE:10-15 (2015) and were taken as 150 for compressed leg members, 200 for other compressed bars and 250 for bars under tension. Finally, the allowable relation w_f/t_{max} follows the recommendations of ASCE:10-15 (2015) and was taken as 25.

A penalization scheme is used to transform the constrained optimization problem given by Eq. 1 into an unconstrained problem. Hence, the objective function (weight) of unfeasible solutions are penalized by a parameter P_t . It is important to carefully choose the penalization in order to avoid convergence issues of the search algorithm. Taking P_t too high can prevent the convergence of the algorithm, while taking it too small may not be enough to avoid unfeasible solutions. For this reason, the penalization is defined as a function of overall constraint violation, according Equation 2:

$$\begin{aligned}
P_t(\mathbf{x}) = h \left[\sum_{i=1}^{m} \left(\frac{|S_{di}(\mathbf{x}) - R_{di}|}{\bar{\sigma}_i} \right)^+ + \right] \\
\left[+ \sum_{i=1}^{m} \left(\frac{|\lambda_i(\mathbf{x}) - \bar{\lambda}_i|}{\bar{\lambda}_i} \right)^+ + \sum_{i=1}^{m} \left(\frac{\frac{w_{fi}(\mathbf{x})}{t_i(\mathbf{x})} - \frac{w_f}{t_{max}}}{\frac{w_f}{t_{max}}} \right)^+ \right]
\end{aligned} \tag{2}$$

where h is a positive constant parameter, with value 10^8, characterizing a technique of constraint handling called death penalty (i.e. the designs outside the admissible domain are excluded from search) Mezura-Montes and Coello (2011).

As previously mentioned, due to the discrete variables and the non-convex and nonlinear characteristic of this optimization problem, the metaheuristic algorithm BSA was employed in order to perform the optimization.

5.1 Optimization algorithm - BSA: Backtracking Search Alogorithm

The BSA is multi-agent based evolutionary algorithm developed by Civicioglu (2013), able to solve unconstrained non-convex optimization problems. It is thus employed in this study to address the optimization problems. A general overview of the BSA is illustrated in Table 1 and the details of each step are in the next subsections. The BSA description shown here is different from the original description given by Civicioglu (2013). The author hope that the description given here be more direct and easy to understand.

Table 1: BSA pseudo-code

```
1. Initialization
Do
  Generation of the perturbed/trial population
      2. Evaluation of the direction/length of the perturbation
      3. Perturbation of the current population
  end
  4. Selection of the new population
Until Stop criteria are met
```

- Initialization

  The initial population P of BSA is generated as defined Equation 3:

$$(P)_{ij} \sim U(x_j^{min}, x_j^{max}) \tag{3}$$

  where U is a random variable uniformly distributed, x_j^{min} and x_j^{max} are the lower and upper bounds of the j^{th} design variable. $i = 1, \ldots, t_{pop}$ and $j = 1, \ldots, n_v$, where t_{pop} represents the size of the population and n_v the dimension of the problem. Thus, each row of P represents an individual of the population and each column represents a design variable. After the construction of the initial population the iterative process of the algorithm is initiated by generating trial populations and updating them until some convergence criterion is achieved.

- Construction of the trial population P_{pert}

  The first step in the construction of the perturbed population (or trial population) P_{pert} is the evaluation of the *direction* of the perturbation that will be applied to the current population. Such a direction is calculated with the aid of the historical population P_{hist}. There are two possible cases for the evaluation of P_{hist}, each with a 50% of chance of happening. In case 1, P_{hist} is generated by a random permutation of the lines of the current population, while in case 2, it is randomly generated just as the initial population. This procedure is illustrated in Table 2, where a and b are random constants following a uniform distribution between zero and one, and $:=$ is an update operator. The author that proposed the BSA claimed that it has a memory from past iterations. Actually, this memory is due to the construction of P_{hist} using case 1. With P_{hist} at hand, the perturbed population P_{pert} is determined according to Equation 4:

Table 2: Evaluation of P_{hist}

if $a < b \,\vert\, a, b \sim U(0,1)$	
then	
$\mathbf{P}_{hist} := \mathbf{P}$	—1st case: $\mathbf{P}_{hist}$ is the random
	— permutation of the lines
$\mathbf{P}_{hist} := randperm(P_{hist} :)$	— of the current **P**
else	
$(P_{old})_{ij}\ U(lb_j, ub_j)$	— 2nd case: $\mathbf{P}_{hist}$ is randomly
	— restarted
end	

$$P_{pert} = P + M.*[\alpha(P_{hist} - P)] \tag{4}$$

in which the operator $.*$ holds for the multiplication term by term and α is a random parameter that controls the amplitude of the search direction matrix $(P_{hist} - P)$. In the present study, α is generated through Equation 5:

$$\alpha = 3N \tag{5}$$

where N is a standard normal random variable (mean equal to zero and standard deviation equal to one). The purpose of the matrix M in Equation 4 is to define which terms of P are perturbed by $\alpha(P_{hist} - P)$ to generate the perturbed or trial population. That is, it is comprised by zeros and ones, and each term M_{ij} of M equal to one means that the corresponding term P_{ij} of P will be perturbed for the construction of the perturbed population P_{pert}

Initially, **M** is set as a $t_{pop} \times n_v$ zero matrix, and for the rest of its construction two cases may be applied at each iteration of the algorithm, each with a 50% chance of happening. In the first case, the parameter mix rate (m_r) chooses randomly up to m_r elements of each line of **M** to assume the unit value. In the second case, only one term of each line is randomly chosen to be equal to 1. The process just described for the construction of **M** is also illustrated in Table 3, in which $randi(n_v)$ is a discrete uniform random value between one and n_v.

As a result of the perturbation process some individuals of the perturbed population may extrapolate the boundaries of the design domain. Thus, at the end of this step, the individuals beyond the search-limits are randomly regenerated in the admissible design domain.

Table 3: Generation of matrix M

$\mathbf{M} = zeros(t_{pop}, n_v)$	
if $a < b \,|\, a, b \sim U(0,1)$	—
then	—**Case 1**: $(m_r\ U\ n_v)$
for $i = 1 : t_{pop}$	— individual are perturbed
$\mathbf{M}_{i,u_{(1:\{mr\,U\,nv\})}} = 1 \,|$ $u = randperm(\{1, 2, 3, \ldots, n_v\})$	—
end	
else	—
for $i = 1 : t_{pop}$	—**Case 2**: only
$\mathbf{M}_{i,u_{randi(nv)}} = 1$	— 1 variable is perturbed
end	—
end	

- Selection of the new population

  In this step, the fitness value of each individual of the perturbed population P_{pert} is evaluated. Then, the algorithm compares the objective value of the the i^{th} individual $(P_{pert})_{(i,:)}$ of the perturbed population to the i^{th} individual $(P)_{(i,:)}$ of P. If the objective function of $(P_{pert})_{(i,:)}$ is better than the one of $(P)_{(i,:)}$, the latter is replaced by the former in the new population of the algorithm.

When the maximum number of iterations (also called *Searches*, defined by parameter S) is reached, the process stops, providing as final results the last best individual and objective function.

6 NUMERICAL EXAMPLES

The Towers 1 and 2, used as numerical examples, are presented in Fig. 6. The steel for profiles is the ASTM A572 G50 and the bolts are M12.

During the optimization the structures are submitted to two different load cases, presented on Fig. 7. Where the constraints (Eq. 2) must be respected on both cases. As mentioned on Section 5, the size optimization is performed by choosing a profile from a discrete set of options. The available profiles, as well as its geometrical properties, are shown on Fig. 8.

It is possible to observe on the available literature, regarding the subject of truss optimization (cited on Section 1), that the size and shape optimization leads to better results, in comparison to the size optimization. Thus, on this paper, only results for size and shape optimization are presented.

6.1 Structure 1

The members of the structure 1, presented in Fig. 6 (a), are divide into thirty five groups, creating thirty five size variables. In order to optimize the structural shape, three geometrical variations are allowed, shown in Fig 9. *Var. 1* is applied horizontally in the four base nodes, *Var. 2* is applied horizontally into top nodes, and *Var. 3* is applied vertically in the tower waist

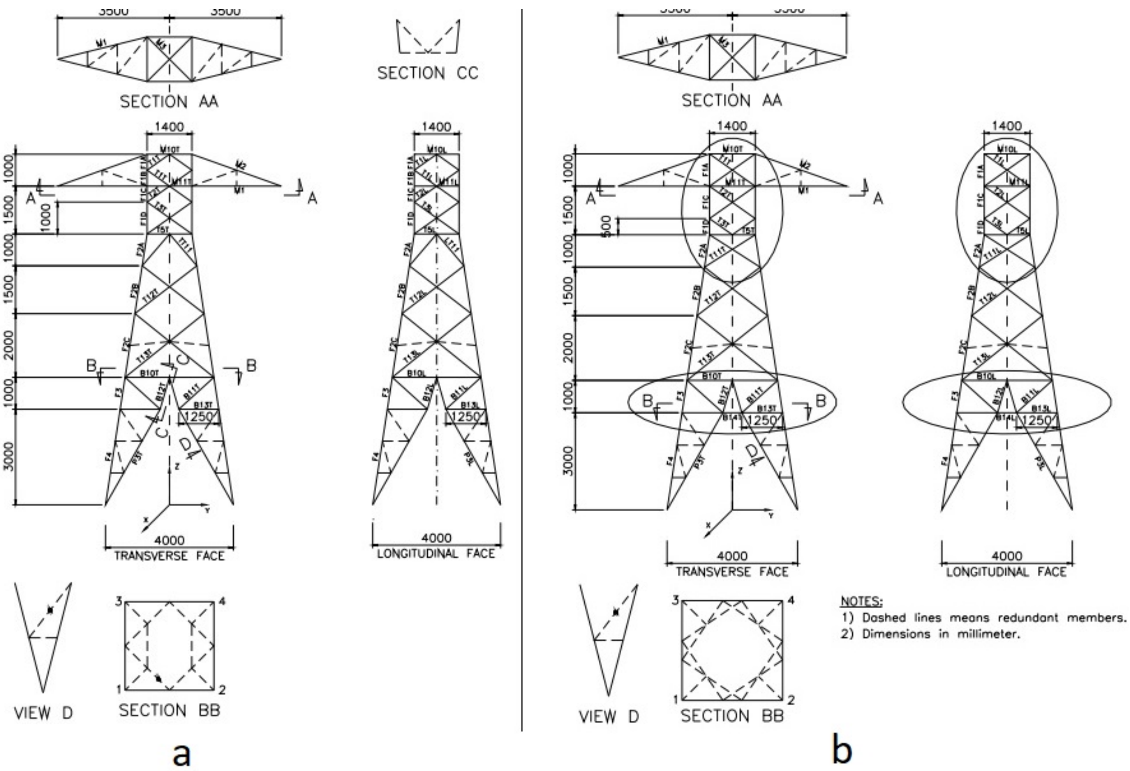

Figure 6: Designs of (a) Structure 1 and (b) Structure 2

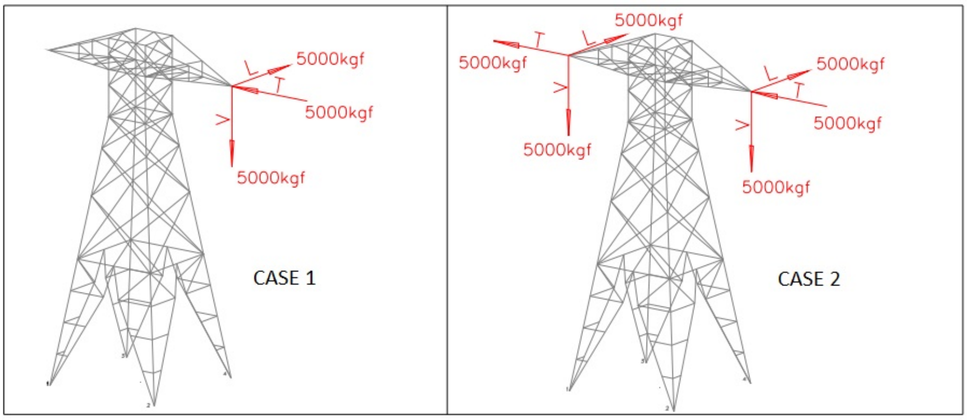

Figure 7: Load cases 1 and 2

(division between the inclined and straight part). The node receiving load are not allowed to move.

The vector **x** is now written as $\mathbf{x} = \{a_1, \ldots, a_{35}, \xi_1, \xi_2, \xi_3\}$, where ξ_q corresponds to variations 1, 2 and 3 of Fig. 9. The lower and upper bound for variations 1, 2 and 3 are: $[-0.20, 0.20]m$; $[-0.10, 0.10]m$ and $[-0.20, 0.20]m$ respectively. The BSA parameters were set as $S = 6000$ and $P = 30$, resulting in 180,000 objective function evaluations (OFE).

The results for this case are presented in Table 4, where the best result found was 1192.41 kg, mean value and standard deviation for ten independent runs of 1193.24 kg and 1.53 kg, respectively. Figure 10 (a) presents the layout of the best result found. It is possible to observe

Size and Thickness (mm)	Weight kg/m	Área cm^2	Axis X-X / Y-Y				Axis Z-Z	B/T
			I cm^4	S cm^3	r cm	e_x cm		
L 40 X 40 X 3.0	1.84	2.35	3.45	1.18	1.21	1.07	0.78	10.33
L 40 X 40 X 5.0	2.97	3.79	5.43	1.91	1.2	1.16	0.77	5.8
L 45 X 45 X 3.0	2.09	2.66	4.93	1.49	1.36	1.18	0.88	11.67
L 45 X 45 X 5.0	3.38	4.3	7.84	2.43	1.35	1.28	0.87	6.6
L 50 X 50 X 5.0	3.77	4.8	11	3.05	1.51	1.4	0.97	7.6
L 50 X 50 X 6.0	4.47	5.69	12.8	3.61	1.5	1.45	0.97	6.17
L 65 X 65 X 5.0	4.95	6.31	24.7	5.21	1.98	1.76	1.28	10.2
L 65 X 65 X 6.0	5.91	7.53	29.2	6.21	1.97	1.8	1.27	8.33
L 75 X 75 X 5.0	5.78	7.36	38.6	7.01	2.29	1.99	1.48	12
L 75 X 75 X 6.0	6.87	8.75	45.6	8.35	2.28	2.04	1.47	9.83
L 75 X 75 X 8.0	9.03	11.5	58.9	11	2.26	2.13	1.45	7.12
L 90 X 90 X 6.0	8.3	10.6	80.3	12.2	2.76	2.41	1.78	12.17
L 90 X 90 X 7.0	9.58	12.2	92.4	14.1	2.75	2.46	1.77	10.28

Figure 8: Available profiles for the size optimization

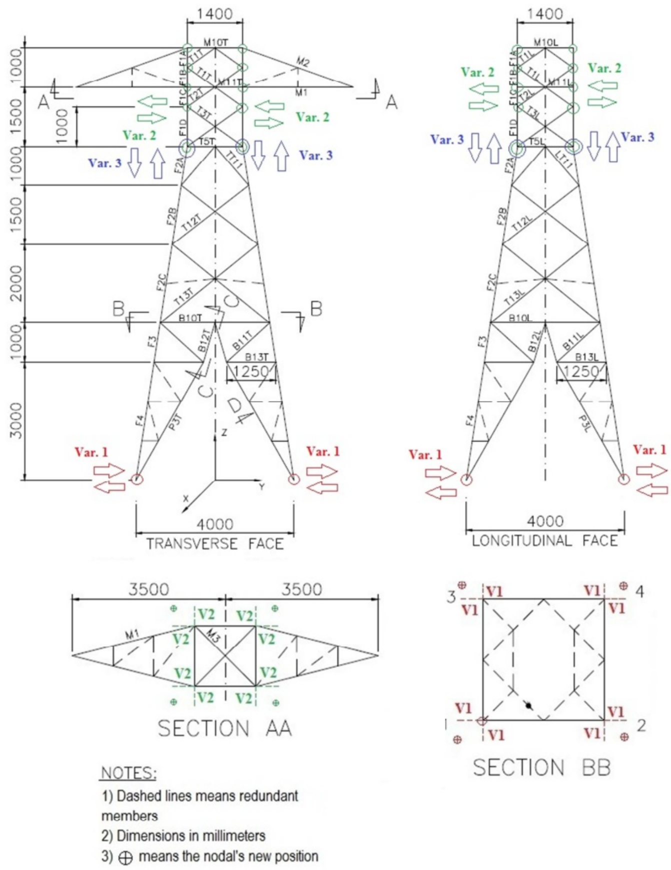

Figure 9: Allowed shape variation for the size optimization

the strong tendency of the structure to be horizontally shortened, where Var. 1 and Var. 3 achieved values on their lower bounds.

Table 4: Results for the size and shape optimization of the Structure 1 without bolt slippage effect

GROUP	Area (cm)	GROUP	Area (cm)	VAR.	(cm)
B10L	2.35E-04	**M11T**	8.75E-04	**Var. 1**	-0.20
B10T	2.35E-04	**P3L**	4.80E-04	**Var. 2**	-0.04
B11L	2.66E-04	**P3T**	2.66E-04	**Var. 3**	-0.20
B11T	2.35E-04	**T1L**	2.35E-04		
B12L	2.66E-04	**T1T**	4.30E-04		
B12T	2.35E-04	**T2L**	4.30E-04		
B13L	2.35E-04	**T2T**	4.80E-04		
B13T	2.35E-04	**T3L**	4.30E-04		
F1	6.31E-04	**T3T**	4.30E-04		
F2	1.06E-03	**T5L**	4.30E-04		
F3	1.06E-03	**T5T**	2.66E-04		
F4	1.06E-03	**LT11**	6.31E-04		
M1	8.75E-04	**TT11**	4.80E-04		
M2	6.31E-04	**T12L**	4.80E-04		
M3	2.35E-04	**T12T**	4.30E-04		
M10L	2.35E-04	**T13L**	5.69E-04		
M10T	4.80E-04	**T13T**	4.80E-04		
M11L	2.35E-04				
Total weight (Kg)	1192.41				
Average* (kg)	1193.24				
S.D.*(kg)	1.53				

***Statistical results for 10 runs.**

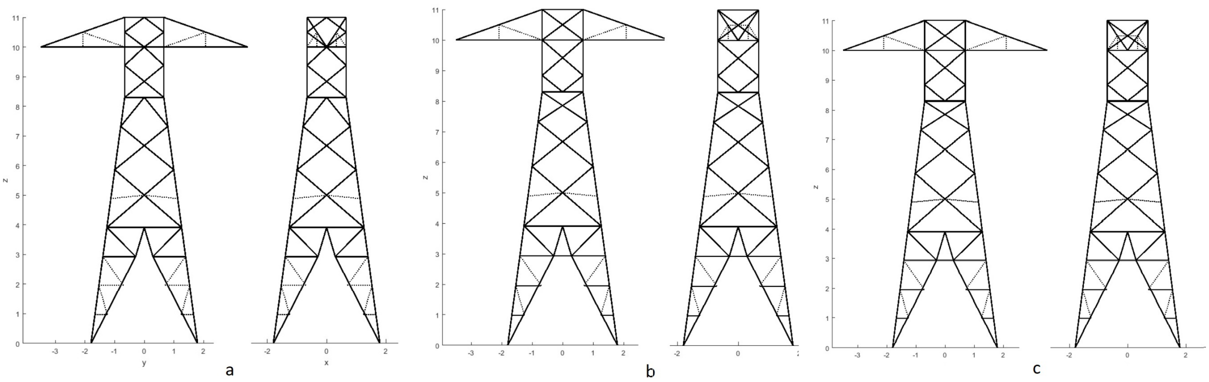

Figure 10: Best result found for the (a) size and optimization of Structure 1 without bolt slippage effect; (b) size and optimization of Structure 2 without bolt slippage effect and (c) size and optimization of Structure 2 with bolt slippage effect

6.2 Structure 2

The procedure presented so far is reproduced for the structure 2, shown on Fig. 6 (b). The members are now divided into thirty seven groups, leading to a vector $\mathbf{x} = \{a_1, \ldots, a_{37}, \xi_1, \xi_2, \xi_3\}$.

Figure 6 (b) highlights the differences between the two designs. Where, the most important discrepancy regards the position of the diaphragm and the inclusion of the members **B14T** and **B14L**. As previously mentioned, although these differences are slight, they play an important role in rigidity of the structure. Consequently, on the importance of the bolt slippage effect.

For this structure two cases are studied: (i) size and shape optimization without the bolt slippage effect, and (ii) size and shape optimization with the bolt slippage effect.

Size and shape optimization without the bolt slippage effect

On this case, the parameters for the size and shape optimization, as well as, for the BSA, are kept unchanged from the *Structure 1* example.

The results for this case are shown in Table 5. Where, the best result found was 1224.15 kg. The mean value and standard deviation, for ten independent runs, were 1226.12 kg and 3.54 kg, respectively. Figure 10 (b) presents the layout for the best result found. One can notice a higher standard deviation, in comparison with the previous case, this can be related to the two additional variables employed on Structure 2. The tendency to horizontally shorten the structure is also observed in this case

Table 5: Results for the size ans shape optimization os the Structure 2 without bolt slippage effect

GROUP	**Area** (cm)	**GROUP**	**Area** (cm)	**VAR.**	(cm)
B10L	4.80E-04	**M11L**	2.35E-04	**Var. 1**	-0.20
B10T	4.80E-04	**M11T**	8.75E-04	**Var. 2**	-0.03
B11L	6.31E-04	**P3L**	5.69E-04	**Var. 3**	-0.20
B11T	5.69E-04	**P3T**	4.80E-04		
B12L	2.35E-04	**T1L**	2.35E-04		
B12T	2.35E-04	**T1T**	3.79E-04		
B13L	2.35E-04	**T2L**	4.30E-04		
B13T	2.35E-04	**T2T**	4.30E-04		
B14L	2.35E-04	**T3L**	4.30E-04		
B14T	2.35E-04	**T3T**	4.30E-04		
F1	6.31E-04	**T5L**	4.30E-04		
F2	1.06E-03	**T5T**	3.79E-04		
F3	8.75E-04	**T11L**	4.30E-04		
F4	8.75E-04	**T11T**	2.66E-04		
M1	8.75E-04	**T12L**	4.80E-04		
M2	4.80E-04	**T12T**	4.30E-04		
M3	2.35E-04	**T13L**	6.31E-04		
M10L	2.66E-04	**T13T**	4.80E-04		
M10T	5.69E-04				
Total weight (Kg)	1224.15				
Average* (kg)	1226.12				
S.D.*(kg)	3.54				

***Statistical results for 10 runs.**

Size and shape optimization with the bolt slippage effect

On this case, the size and shape variations and the BSA parameters follow the previous cases. However, the mechanical model now considers the bolt slippage effects. Which are described in Section 3.

It is important to point out that, since the consideration of the bolt slippage effect demands a iterative process, the computation cost is significantly increased. Additionally, due to the random aspect of the optimization algorithm, the first generations of searches (performed by the BSA), can create ill conditioned designs. Finally, the construction of the model with bolt slippage, as mentioned on Section 3.1, requires the number of bolts. However, the last is evaluated using the stresses obtained from the model solution, creating a circular reference. To overcome these drawbacks, the optimization process is divided into two phases, illustrated in the flowchart on Fig. 11.

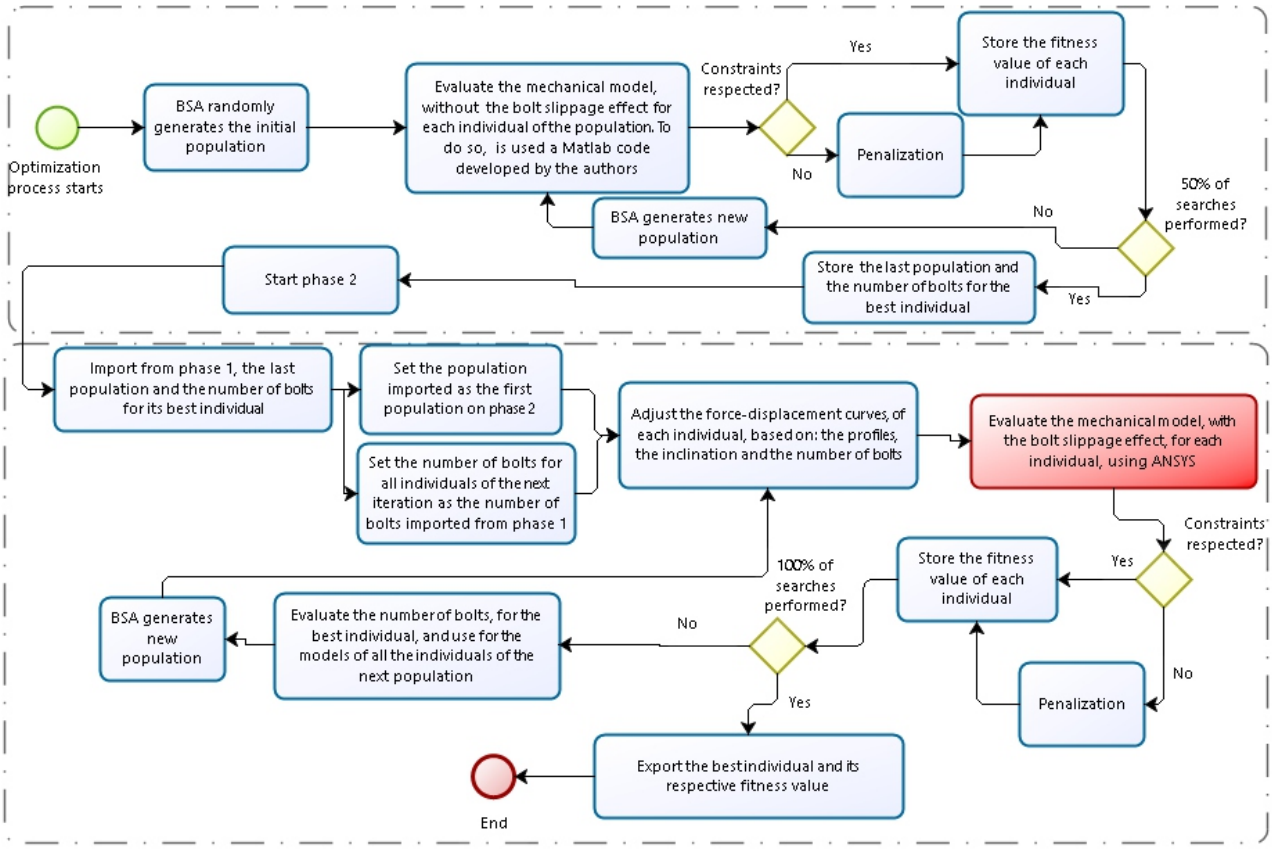

Figure 11: Flowchart of the optimization scheme when the bolt slippage is considered

- On **phase 1**, 50% of the searches are evaluated, and the model does not considers the bolt slippage effect, i.e. exactly as the previous examples. Furthermore, the final population and the number of bolts for the best individual are saved.
- On **phase 2**, the remaining 50% evaluations are performed considering the bolt slippage effect. Where, the initial population of the BSA on phase 2, instead of being randomly generated, is set as the last population provided by phase 1. Additionally, the number of bolts used in a given iteration, is the one evaluated for the best individual of the last

iteration. For the first iterations on phase 2, it is used the number of bolts saved from phase 1. Through this process, and assuming a low diversity on the final populations, it is expected that the best result found is evaluated with the correct number of bolts.

As described in Section 3.1, the mechanical model with bolt slippage effect is evaluated using ANSYS, this task is highlighted in red on Fig. 11. Yet, the evaluation of the mechanical model without bolt slippage effect (as well as all other processes, are performed in Matlab)

Figure 10 (c) presents the layout of the best result found for this case. The results, including the number of bolts for the best design, are presented in Table 6. The best result found was 1166.55 kg, with mean value and standard deviation, for 10 independent runs, of 1171.94 kg 5.11 kg. The higher standard deviation indicates that the consideration of the bolt slippage effect increases the variability of the independent runs. The tendency to horizontally shorten the structure was again observed. The best result found for this case is 2.17% lighter in comparison with the size and shape optimization of Structure 1 without bolt slippage effect.

Table 6: Results for the size ans shape optimization os the Structure 2 with bolt slippage effect

GROUP	**Area** (cm)	**BOLTS**	**GROUP**	**Area** (cm)	**BOLTS**	**VAR.**	(cm)
B10L	2.66E-04	2	**M11L**	2.35E-04	2	**Var. 1**	-0.20
B10T	2.66E-04	2	**M11T**	8.75E-04	4	**Var. 2**	0.00
B11L	2.66E-04	2	**P3L**	4.30E-04	2	**Var. 3**	-0.20
B11T	2.35E-04	2	**P3T**	4.30E-04	2		
B12L	2.35E-04	2	**T1L**	2.35E-04	2		
B12T	2.35E-04	2	**T1T**	2.66E-04	4		
B13L	2.35E-04	2	**T2L**	4.30E-04	4		
B13T	2.35E-04	2	**T2T**	4.30E-04	4		
B14L	2.35E-04	2	**T3L**	3.79E-04	2		
B14T	2.35E-04	2	**T3T**	3.79E-04	2		
F1	6.31E-04	4	**T5L**	3.79E-04	2		
F2	1.06E-03	10	**T5T**	2.66E-04	4		
F3	1.06E-03	12	**T11L**	4.30E-04	2		
F4	1.06E-03	12	**T11T**	2.66E-04	4		
M1	8.75E-04	8	**T12L**	4.80E-04	2		
M2	4.80E-04	6	**T12T**	4.30E-04	2		
M3	2.35E-04	2	**T13L**	5.69E-04	2		
M10L	2.66E-04	2	**T13T**	4.80E-04	2		
M10T	3.79E-04	4					
Total weight (Kg)	1166.52						
Average* (kg)	1171.94						
S.D.*(kg)	5.11						

***Statistical results for 10 runs.**

7 CONCLUSIONS

In this paper it is presented the size and shape optimization of two transmission line structures, submitted to two load cases and with stress and slenderness constraints, evaluated following the recommendations of ASCE:10-15 (2015). Employing the Backtracking Search Algorithm (BSA).

The results show a strong tendency, in all cases studied, to horizontally shorten the structure. Additionally, it is possible to observer an increase on the standard deviation along the studied cases. This can be related to higher complexity of the model with bolt slippage effect and also to the higher number of variables on Structure 2.

One can notice that the best result found for the size and shape optimization, with bolt slippage effect, of the Structure 2, lead to a 2.17% better design in comparison to the size and shape optimization, without bolt slippage effect, of the Structure 1. Although 2.17% is a small reduction, this is a promising result, because indicates that a more complex (and costly) analysis can payoff, leading to a best overall result.

Additionally, the strategy to address the number of bolts on the optimization with bolt slippage effect also presented promising results. Since, on all final designs, the model employed the correct number of bolts.

It is important to highlight that several further studies are necessary, in order to better understand the behavior of the connections and how its affected by the tower configuration. Finally, despite the promising results presented in this paper, more examples employing full-scale transmission towers with different configurations, are required to achieve more comprehensible conclusions.

ACKNOWLEDGEMENTS

The authors gratefully knowledge CAPES and CNPq.

References

Ahmed, K. I. (2007). Finite element modeling of non-linear structural response of transmission towers including bolted joint slippage. *University of British Columbia*.

Al-Bermani, F. G. and Kitipornchai, S. (1990). Nonlinear analysis of thin-walled structures using least element/member. *Journal of structural engineering*, 116(1):215–234.

ASCE:10-15 (2015). *ASCE 10:15*. American Society of Civil Engineers.

Camp, C. and Farshchin, M. (2014). Design of space trusses using modified teachinglearning based optimization. *Engineering Structures*, 6263:87 – 97.

CIGRE (1991). *CIGR Brochure 138*. Conseil International des Grands Rseaux Electriques, Paris.

CIGRE (2009). *CIGR Brochure 387*. Conseil International des Grands Rseaux Electriques, Paris.

Civicioglu, P. (2013). Backtracking search optimization algorithm for numerical optimization problems. *Applied Mathematics and Computation*, 219(15):8121–8144.

de Souza, R. R., Miguel, L. F. F., Lopez, R. H., Miguel, L. F. F., and Torii, A. J. (2016). A procedure for the size, shape and topology optimization of transmission line tower structures. *Engineering Structures*, 111:162–184.

Dobbs, M. W. and Felton, L. P. (1969). Optimization of truss geometry. *Journal of the Structural Division*, 95(10):2105–2118.

Dorn, W. S. (1964). Automatic design of optimal structures. *Journal de mecanique*, 3:25–52.

Galante, M. (1996). Genetic algorithms as an approach to optimize real-world trusses. *International Journal for Numerical Methods in Engineering*, 39(3):361–382.

Goldberg, D. E. and Samtani, M. P. (1986). Engineering optimization via genetic algorithm. In *Electronic Computation (1986)*, pages 471–482. ASCE.

Grierson, D. and Pak, W. (1993). Optimal sizing, geometrical and topological design using a genetic algorithm. *Structural Optimization*, 6(3):151–159.

Guo, H. and Li, Z. (2011). Structural topology optimization of high-voltage transmission tower with discrete variables. *Structural and Multidisciplinary Optimization*, 43(6):851–861.

Hajela, P. and Lee, E. (1995). Genetic algorithms in truss topological optimization. *International journal of solids and structures*, 32(22):3341–3357.

Hemp, W. S. (1973). *Optimum structures*. Clarendon Press.

Kaminski-Jr, J. (2007). Incertezas de modelo na análise de torres metálicas treliçadas de linhas de transmissão. *UFRGS*.

Kaveh, Gholipour, and Rahami (2008). Optimal design of transmission towers using genetic algorithm and neural networks. *International Journal of Space Structures*, 23(1):1–19.

Kelesoglu, O. (2007). Fuzzy multiobjective optimization of truss-structures using genetic algorithm. *Advances in Engineering Software*, 38(10):717–721.

Kitipornchai, S., Al-Bermani, F., and Peyrot, A. (1994). Effect of bolt slippage on ultimate behavior of lattice structures. *Journal of Structural Engineering*, 120(8):2281–2287.

Kroeker, D. (2000). *Structural analysis of transmission towers with connection slip modeling*. PhD thesis, University of Manitoba.

Mathakari, S., Gardoni, P., Agarwal, P., Raich, A., and Haukaas, T. (2007). Reliability-based optimal design of electrical transmission towers using multi-objective genetic algorithms. *Computer-Aided Civil and Infrastructure Engineering*, 22(4):282–292.

Mezura-Montes, E. and Coello, C. A. C. (2011). Constraint-handling in nature-inspired numerical optimization: past, present and future. *Swarm and Evolutionary Computation*, 1(4):173–194.

Miguel, L. F. F., Lopez, R. H., and Miguel, L. F. F. (2013). Multimodal size, shape, and topology optimisation of truss structures using the firefly algorithm. *Advances in Engineering Software*, 56:23–37.

NBR:8850 (2003). *NBR 8850*. Associação Brasileira de Normas Técnicas, Rio de Janeiro.

Noilublao, N. and Bureerat, S. (2011). Simultaneous topology, shape and sizing optimisation of a three-dimensional slender truss tower using multiobjective evolutionary algorithms. *Computers & Structures*, 89(23):2531–2538.

Pedersen, P. (1972). On the optimal layout of multi-purpose trusses. *Computers & Structures*, 2(5):695–712.

Rahami, H., Kaveh, A., and Gholipour, Y. (2008). Sizing, geometry and topology optimization of trusses via force method and genetic algorithm. *Engineering Structures*, 30(9):2360 – 2369.

Rajan, S. (1995). Sizing, shape, and topology design optimization of trusses using genetic algorithm. *Journal of Structural Engineering*.

Rajeev, S. and Krishnamoorthy, C. (1992). Discrete optimization of structures using genetic algorithms. *Journal of structural engineering*.

Shea, K. and Smith, I. F. (2006). Improving full-scale transmission tower design through topology and shape optimization. *Journal of structural engineering*, 132(5):781–790.

Šilih, S., Kravanja, S., and Premrov, M. (2010). Shape and discrete sizing optimization of timber trusses by considering of joint flexibility. *Advances in Engineering Software*, 41(2):286–294.

Sivakumar, P., Rajaraman, A., Samuel Knight, G., and Ramachandramurthy, D. (2004). Object-oriented optimization approach using genetic algorithms for lattice towers. *Journal of computing in civil engineering*, 18(2):162–171.

Sved, G. and Ginos, Z. (1968). Structural optimization under multiple loading. *International Journal of Mechanical Sciences*, 10(10):803–805.

Tang, W., Tong, L., and Gu, Y. (2005). Improved genetic algorithm for design optimization of truss structures with sizing, shape and topology variables. *International Journal for Numerical Methods in Engineering*, 62(13):1737–1762.

Torii, A. J., Lopez, R. H., and Biondini, F. (2012). An approach to reliability-based shape and topology optimization of truss structures. *Engineering Optimization*, 44(1):37–53.

Torii, A. J., Lopez, R. H., and Miguel, L. F. F. (2014). Modeling of global and local stability in optimization of truss-like structures using frame elements. *Structural and Multidisciplinary Optimization*, 51(6):1187–1198.

Tort, C., Şahin, S., and Hasançebi, O. (2017). Optimum design of steel lattice transmission line towers using simulated annealing and pls-tower. *Computers & Structures*, 179:75–94.

Ungkurapinan, N., Chandrakeerthy, S. D. S., Rajapakse, R., and Yue, S. (2003). Joint slip in steel electric transmission towers. *Engineering Structures*, 25(6):779–788.

Wang, H. and Ohmori, H. (2013). Elasto-plastic analysis based truss optimization using genetic algorithm. *Engineering Structures*, 50:1–12.

Wu, S.-J. and Chow, P.-T. (1995). Integrated discrete and configuration optimization of trusses using genetic algorithms. *Computers & structures*, 55(4):695–702.